Journal of Superconductivity and Novel Magnetism (2020) 33:1851–1857
https://doi.org/10.1007/s10948-020-05439-9

ORIGINAL PAPER

Magnetism and Magnetocaloric Efffects of R_3Pd_4 (R = Nd and Pr) Compounds

Z. X. Yang[1] · Y. J. Wang[2] · X. F. Wu[2] · Y. S. Du[2] · S. Cang[1] · J. Q. Deng[2] · L. Ma[2] · J. Wang[2]

Received: 17 October 2019 / Accepted: 22 January 2020 / Published online: 4 February 2020

Abstract

The magnetic properties and magnetocaloric effects of the intermetallic compounds R_3Pd_4 (R = Nd and Pr) were investigated. The results show that the ground state of the Nd_3Pd_4 compound is weakly antiferromagnetic below the Néel temperature T_N of 9.4 K, which can be induced to be ferromagnetic state with a small applied field. For the Pr_3Pd_4 compound, it does not show any magnetic order-disorder transition down to 5 K. In the paramagnetic region, the reciprocal magnetic susceptibilities χ^{-1} for both compounds obey the Curie-Weiss law. The values of the effective magnetic moment for R_3Pd_4 (R = Nd and Pr) are determined to be 3.83 μ_B/Nd^{3+} and 3.51 μ_B/Pr^{3+}, respectively, and the corresponding paramagnetic Curie temperatures were determined to be 6.5 K and − 17 K. For a magnetic field change of 0–5 T, the maximum magnetic entropy changes ($-\Delta S_M$) for Nd_3Pd_4 and Pr_3Pd_4 are found to be 7.8 J/kg K and 6.9 J/kg K, respectively. The corresponding value of refrigerant capacity (RC) for the Nd_3Pd_4 compound is estimated to be 74 J/kg.

Keywords R_3Pd_4 (R = Nd and Pr) compounds · Metamagnetic transition · Magnetocaloric effect

1 Introduction

The temperature of material increases or decreases when applied or removed an external magnetic field adiabatically, and this phenomenon is called the magnetocaloric effect (MCE). Magnetic refrigeration based on the MCE is expected to be a promising cooling technique, which might replace the conventional gas compression refrigeration due to its higher energy efficiency and greater environmental friendliness [1–4]. The MCE is an intrinsic property of magnetic materials, which can be characterized by the magnetic entropy change in an isothermal process (ΔS_M) and/or the temperature change in an adiabatic process (ΔT_{ad}) [5, 6]. Besides, the refrigerant capacity (RC), which is characterized by the amount of the heat transfer between the hot and cold sinks in an ideal refrigeration cycle, is considered to be another important and meaningful parameter to evaluate the magnetocaloric properties [7]. In the past decades, a great number of ferromagnetic (FM) materials with first-order magnetic transition (FOMT) from FM to paramagnetic (PM) states have been found to show large MCE around their transition temperatures [8, 9], such as $Mn_{1-x}Fe_xAs$ [10], $ErCo_2$ [11, 12], $Gd_5(Si_{1-x}Ge_x)_4$ [13, 14], and Heulser alloys Ni-Mn-Sn [15]. However, the majority of them are usually accompanied by thermal and magnetic hysteresis losses and result in the irreversibility in $-\Delta S_M$ and ΔT_{ad} curves, which may greatly reduce the effective RC of the magnetic refrigerant materials in a cooling cycle [1, 16, 17]. Therefore, it is of great importance to acquire magnetic materials with a large reversible MCE. Up to now, some antiferromagnetic (AFM) materials have been investigated theoretically and experimentally, such as DyCuSi [1], DySb [18], $ErRu_2Si_2$ [19], and $GdCo_2B_2$ [20]. It was found that these materials possess a giant MCE associated with the first-order magnetic field–induced order-to-order metamagnetic transition from AFM to FM states accompanied by quite small magnetic and thermal hysteresis losses [19, 21, 22]. Consequently, it is desirable to explore the AFM-FM metamagnetic transition material for the practical application in magnetic refrigerant.

The R_3Pd_4 compounds (R = rare earth) have been known for many years. Palenzona and Iandelli firstly reported the

✉ Y. J. Wang
wang_wangyj@163.com

✉ Y. S. Du
duyusong@guet.edu.cn

[1] Key Laboratory of Impact and Safety Engineering, Ministry of Education, Ningbo University, Ningbo 315211, China

[2] School of Materials Science and Engineering, Guangxi Key Laboratory of Information Materials, Guilin University of Electronic Technology, Guilin 541004, China

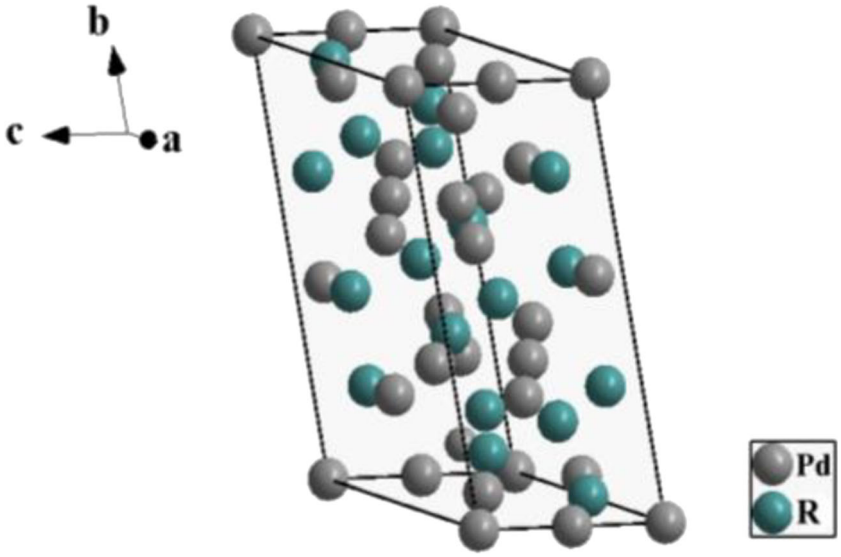

Fig. 1 The unit cell of R_3Pd_4. 1f, -3a, and -3b Wyckoff sites are occupied by Pd atoms and 1f site by R atoms

structure and lattice constants of R_3Pd_4 (R = La-Nd, Y, Sm and Gd-Lu), determining that all the compounds crystallize in a rhombohedral Pu_3Pd_4-type (space group R-3) [23]. The crystal structure of R_3Pd_4 is exhibited in Fig. 1 where the rare earth atoms R occupy only one crystallographic site (1f), while the Pd atoms take up three crystallographic sites: (1f), (-3a) and (-3b). Preliminary magnetic measurements of the R_3Pd_4 compounds were carried out by Yakinthos et al., and they found that the compounds of Nd_3Pd_4, Tb_3Pd_4, Dy_3Pd_4, and Ho_3Pd_4 order antiferromagnetically with the Néel temperatures below 20 K [24]. However, a literature survey shows that apparently the MCEs of the R_3Pd_4 compounds have not been studied in detail. In this paper, the Nd_3Pd_4 and Pr_3Pd_4 compounds were chosen as the object of study and the magnetic properties and magnetocaloric behavior of them were investigated. The observed considerable magnetocaloric effects indicate that Nd_3Pd_4 and Pr_3Pd_4 may be two suitable candidates for magnetic refrigerant in low temperature range with no thermal loss.

2 Experimental

The intermetallic R_3Pd_4 (R = Nd and Pr) compounds were synthesized by arc-melting the constituent elements (ingot, Yosoc Science & Technology Co. Ltd., Beijing, China) with the purity better than 99.99 wt% in a high-purity argon atmosphere on a water-cooled copper crucible. The ingots were turned over and remelted four times to ensure homogeneity. The weight loss less than 0.5 wt% during melting was acceptable. And then both ingots were sealed in the evacuated quartz tubes for isothermal heat treatment at 800 K for 7 days. Subsequently, the samples were quenched to room temperature in ice-water mixture. A portion of each ingot was ground to powder for X-ray diffraction (XRD, PANalytical Empyrean) measurement by using Cu Kα radiation (λ = 1.54056 Å) at room temperature to identify the single-phase nature of the R_3Pd_4 (R = Nd and Pr) compounds. The remaining ingot samples were used to the magnetic measurement by the vibrating sample magnetometer (VSM) option of the physical property measurement system (PPMS-9, Quantum Design, Inc.).

3 Results and Discussion

The XRD patterns at room temperature for Nd_3Pd_4 and Pr_3Pd_4 with 2θ = 20–90°are illustrated in Fig. 2. The vertical bars at the bottom are the calculated Bragg diffraction peaks of the Pr_3Pd_4 phase. Since the characteristic diffraction peaks of the adjacent rare earth elements (Nd and Pr) are basically the same, only Pr_3Pd_4 Bragg diffraction peaks are used to compare in our study [23]. It is clearly observed that the

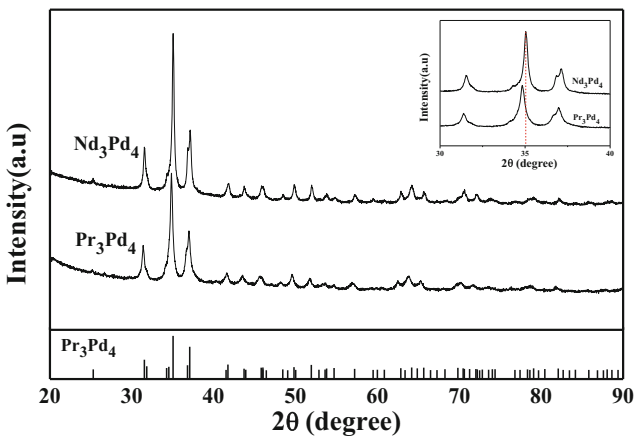

Fig. 2 Powder XRD patterns of Nd_3Pd_4 and Pr_3Pd_4 at room temperature. The calculated diffraction peaks (bottom) of the Pr_3Pd_4 phase with the Pu_3Pd_4-type hexagonal structure

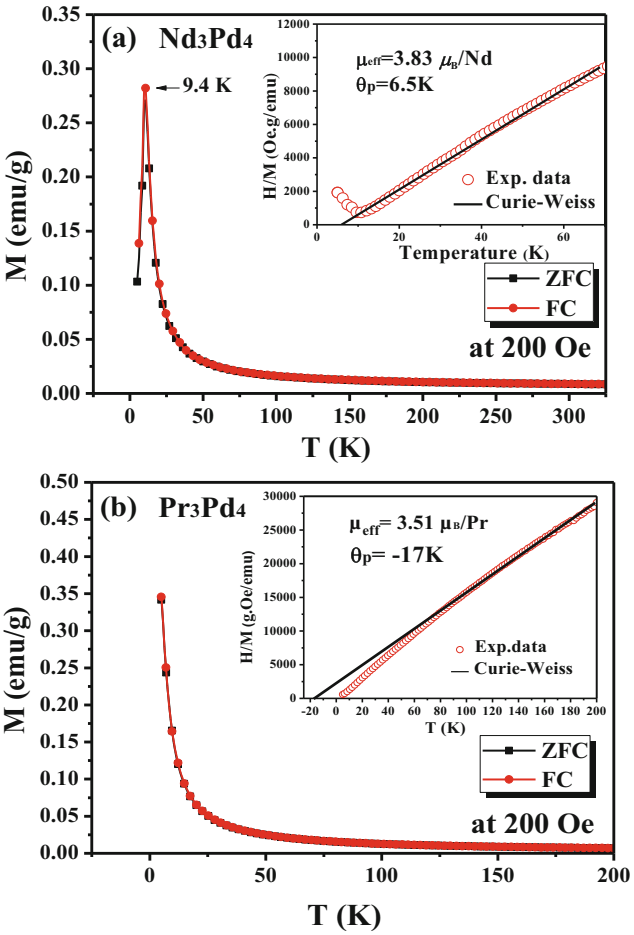

Fig. 3 (color online) Temperature dependences of ZFC and FC magnetizations for **a** Nd_3Pd_4, **b** Pr_3Pd_4 under the magnetic field of 200 Oe; the inset are temperature variation of the inverse dc susceptibility fitted to the Curie-Weiss law, respectively

experimental peaks are consistent with the calculated ones and no redundant peaks are evident, which suggests that both the compounds crystallize in a single phase with the Pu_3Pd_4-type hexagonal structure. The inset of Fig. 2 presents the enlarged main characteristic diffraction peaks of Nd_3Pd_4 and Pr_3Pd_4. It is clear that the positions of the diffraction peaks of Nd_3Pd_4 shift to a higher angle (e.g., in the vicinity of $2\theta = 35°$) compared with those of Pr_3Pd_4, which suggests the lattice constants of R_3Pd_4 compounds decrease due to the lanthanide contraction [23].

Figure 3a shows the temperature dependence of zero-field-cooled (ZFC) and field-cooled (FC) magnetizations for the Nd_3Pd_4 compound in a field of 200 Oe. A typical λ-type peak is observed both in the ZFC and FC curves, revealing that Nd_3Pd_4 experiences an AFM-to-PM magnetic transition at the Néel temperature $T_N = 9.4$ K, which is consistent with the previous report of Yakinthos et al. [24]. The insert of Fig. 3a is the temperature dependence of the inverse of magnetic susceptibility χ^{-1} derived from the FC curve under the field of 200 Oe. In the PM region, the susceptibility shows a Curie-Weiss behavior. The calculation result of the effective magnetic moment (μ_{eff}) is obtained to be 3.83 μ_B/Nd^{3+}, which is slightly larger than the theoretical value of Nd^{3+} (3.62 μ_B). A similar enhancement of the μ_{eff} is also observed in the RNiAl compounds [25, 26] and may be attributed to the polarization of the conduction band, which is termed as magnetic polaronic effect [27, 28]. The paramagnetic Curie temperature (θ_P) is determined to be about 6.5 K, which is smaller than the value of 8 K reported by Yakinthos et al. [24]. Here, it is of interest to note that the observed value of θ_P that represents the sum of all magnetic interactions in system is positive, which seems contradictory to the result derived from the *M-T* curves. Usually, an AFM material exhibits a negative θp value and similar phenomenon also has been observed in some AFM compounds, such as R_2PdSi_3 (R = Tb, Dy) [28], HoNiGa [29], and HoNiAl [25]. The positive θp values indicate the presence of the dominating FM interaction in these compounds, and the AFM ground state in these compounds is unstable and can be easily induced into a FM state by an applied magnetic field [29].

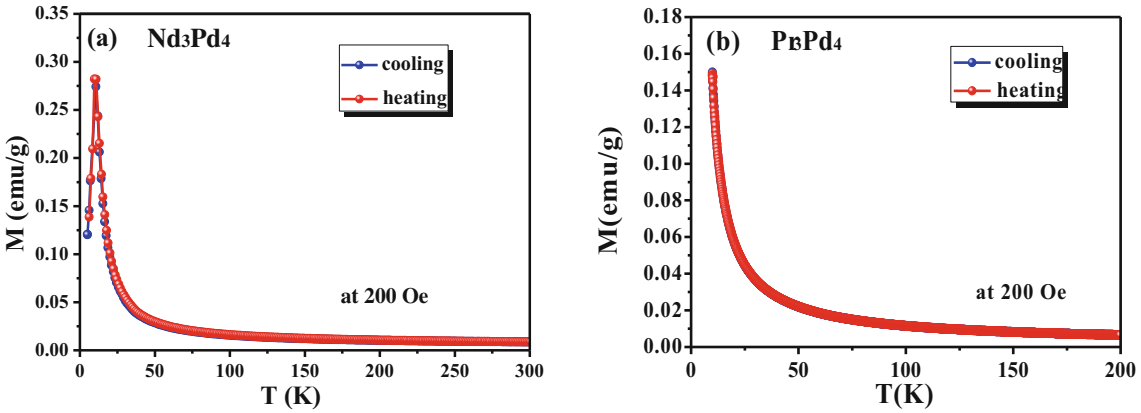

Fig. 4 (color online) Temperature dependences of the magnetizations for **a** Nd_3Pd_4, **b** Pr_3Pd_4 measured on heating and cooling processes in applied magnetic fields of 200 Oe

The temperature dependence of magnetization in the FC and ZFC models for the Pr_3Pd_4 compound in a temperature range of 5–200 K was measured and shown in Fig. 3b. It is observed that the magnetization decreases greatly with increasing temperature indicating there exists a magnetic transition, however, it does not show any magnetic ordering state down to 5 K. Yakinthos et al. [24] studied Pr_3Pd_4 with the temperature as low as 4.2 K, but the ordering state was still not observed. The inset of Fig. 3b is the temperature dependence of the magnetic susceptibility χ^{-1} of Pr_3Pd_4 measured under an applied field of 200 Oe as well as the Curie-Weiss fit. By fitting the high temperature range in the PM region, it is found that the susceptibility mainly obeys the Curie-Weiss law $\chi^{-1} = (T - \theta_P)/C$ with an effective magnetic moment of 3.51 μ_B and a paramagnetic Curie temperature θ_P of − 17 K. The calculated effective magnetic moment 3.51 μ_B is close to the theoretical value of Pr^{3+} (3.58 μ_B) indicating that the Pd atom in the Pr_3Pd_4 compound is probably non-display magnetism. The obtained negative value of θ_P is equal to that of − 17 K reported by Yakinthos et al. [24], which suggests the possible presence of AFM interaction coupling in the Pr_3Pd_4 compound.

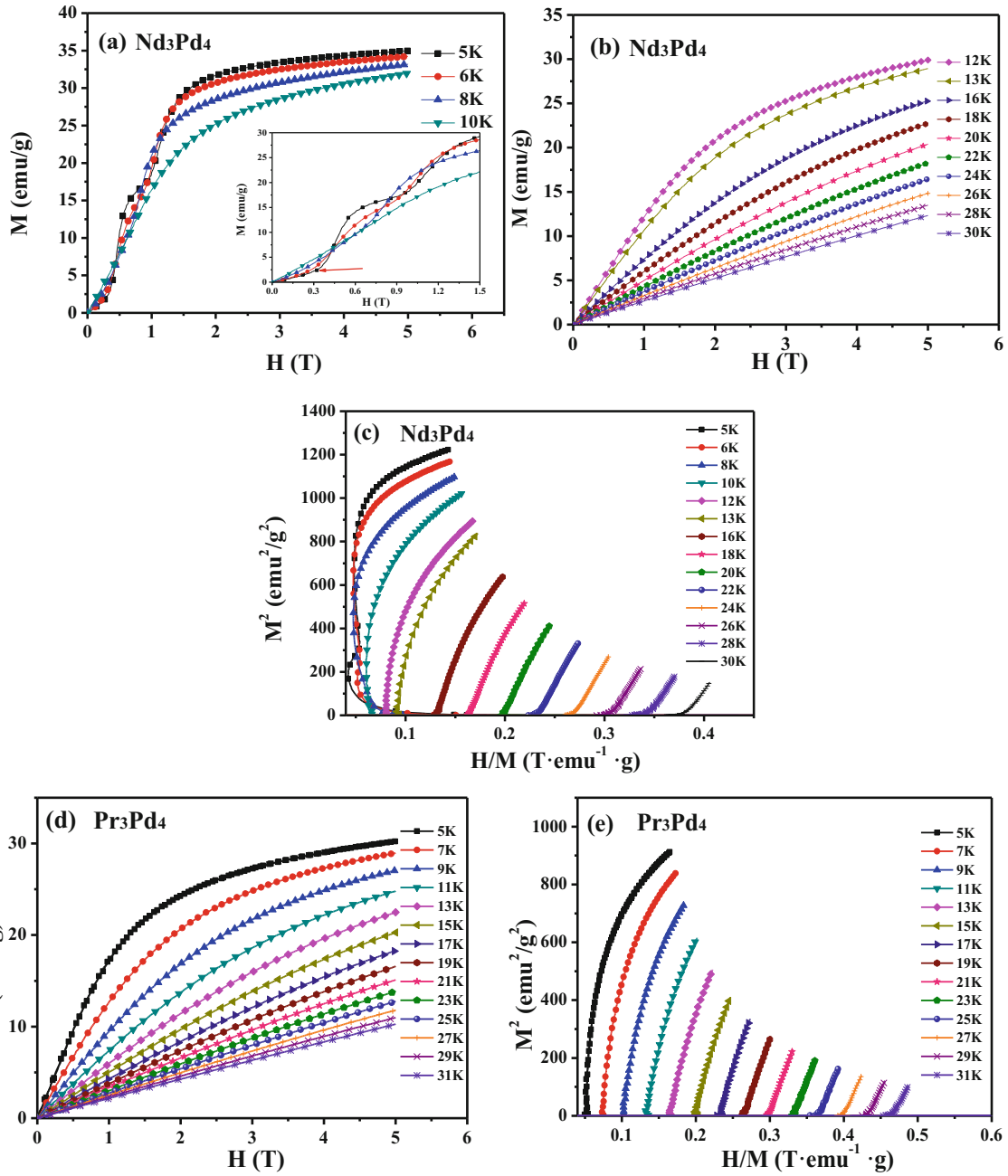

Fig. 5 (color online) Field-dependent magnetizations of **a** and **b** Nd_3Pd_4, **d** Pr_3Pd_4. The inset of **a** shows the magnetization isotherms under low magnetic fields. **c**, **e** Arrott plots of those compounds in the temperature regions of 5–30 K and 5–31 K, respectively

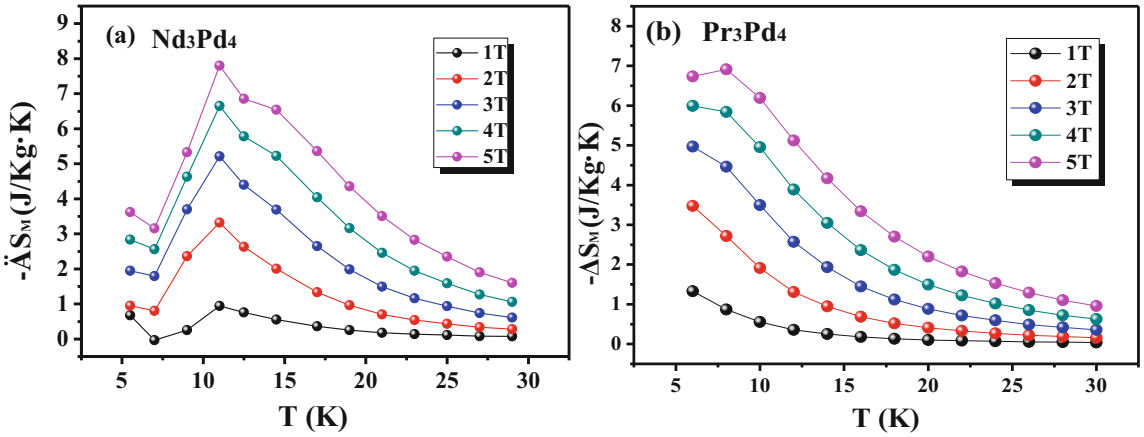

Fig. 6 (color online) Temperature dependence of magnetic entropy change of **a** Nd_3Pd_4 and **b** Pr_3Pd_4 compounds under different magnetic field changes increasing from 1 to 5 T

In order to investigate whether there is thermal hysteresis near the magnetic transition temperature, the magnetizations versus temperature curves of Nd_3Pd_4 and Pr_3Pd_4 under an applied magnetic field of 200 Oe on heating and cooling processes were recorded and shown in Fig. 4a and 4b, respectively. It is found that the heating and cooling curves completely overlap and show a reversible behavior, which is beneficial for the efficiency of the magnetic refrigeration.

Figure 5a displays the magnetization isotherms of Nd_3Pd_4 in a temperature range of 5–10 K under applied fields up to 5 T. The inset of Fig. 5a is the magnetization isotherms under low magnetic fields, where it is observed that for the curves below the T_N, the magnetizations increase linearly at first and the values of magnetization at high temperature are greater than that at low temperature, indicating the nature of the AFM ground state in Nd_3Pd_4. With increasing the magnetic field, the magnetization increases quickly in a step-like jump way leading to a crossover among the magnetization isotherms. This result confirms that the AFM ground state in Nd_3Pd_4 is not stable and can be induced to be the FM state by applying a field, which is in agreement with the positive θp value discussed above. Besides, the magnetization isotherms of Nd_3Pd_4 above T_N are shown in Fig. 5b. An upward bending of the *M-H* curves can be observed, indicating the presence of short-range FM interaction induced by an external magnetic field in the PM state [25, 28] and the *M-H* curves become more and more linear with increase of the temperature. To further confirm the nature of the magnetic transition for Nd_3Pd_4 compound, the slopes of M^2-*H*/*M* (Arrott) curves are shown in Fig. 5c. According to the Banerjee criterion [30], the character of the magnetic transition is expected to be of the first order when the curve shows negative slope or inflection point in the Arrott plot; otherwise, it will be of the second order when the slope is positive. It can be seen from Fig. 5c that the Arrott plots below T_N exhibit negative slopes, confirming that the metamagnetic transition from AFM to FM state is of first order. Besides, the positive slope of Arrott plot above T_N indicates the characteristic of a second-order transition from FM to PM states.

The isothermal magnetization curves (*M-H*) for Pr_3Pd_4 were measured in the temperature range from 5 to 31 K corresponding to the PM state and shown in Fig. 5d. Just like the Nd_3Pd_4 above T_N, there also exist curvatures in the isothermal curves indicating the short-range FM correlations in the PM state induced by the applied field. With increase of the temperature, the curves get more and more linear and the magnetization decreases obviously. Figure 5e presents the Arrott plots of Pr_3Pd_4, it is observed that there only exists positive slope in the PM range, suggesting the nature of a second-order transition from FM to PM states.

The temperature dependence of $-\Delta S_M$ under the applied field change of 0–5 T are shown in Fig. 6a and 6b, which were

Table 1 The main parameters about the MCE for R_3Pd_4 (R = Nd and Pr) and other representative magnetic refrigerant materials in the similar working temperature range. A blank column with "–" mark indicates that the value is not revealed in the literatures

Alloys	T_M(K)	ΔS_M (J/kg K)		RC(J/kg)	Refs.
		0–2 T	0–5 T	0–5 T	
Nd_3Pd_4	9.4	3.3	7.8	94	Present
Pr_3Pd_4	–	3.5	6.9	–	Present
Pr_7Pd_3	15	–	5.5	65	[37]
PrNi	20	2.4	6.1	43	[38]
$NdCo_2B_2$	27	4.5	7.1	80	[39]
Dy_5Ge_4	46	–	6.8	161	[40]
$TbCo_2B_2$	15	–	6.2	–	[41]
TbNiIn	71	2.4	5.3	191	[42]
$PrCo_2B_2$	16	4.9	8.1	–	[43]

evaluated from the *M-H* data by using the thermodynamic Maxwell relation [31] as given in Eq. (1).

$$\Delta S_M(T, \Delta H) = \int_{H_1}^{H_2} \left(\frac{\delta M(T,H)}{\delta T}\right)_H \mathrm{d}H \quad (1)$$

where T and H are the absolute temperature and the applied field, respectively. To derive the numerical of magnetic entropy change, the approximation of the integral can be adopted [32]:

$$\Delta S_M(T, \Delta H) = \sum \frac{M_i - M_{i+1}}{T_i - T_{i+1}} \Delta H_i \quad (2)$$

where M_i and M_{i+1} are the experimental magnetization under the temperature T_i and T_{i+1} in an applied magnetic field H_i. For the Nd_3Pd_4 compound, it can be seen from Fig. 6a that the maxima values of the $-\Delta S_M$ reach to 3.3 J/kg K and 7.8 J/kg K under the applied magnetic fields of 2 T and 5 T, respectively. The maximum occurs around 11 K, and the maxima values of $-\Delta S_M$ increase with the increasing field change. For the Pr_3Pd_4 compound, due to the limited temperature range of our experimental conditions, the magnetic entropy curve is not fully displayed in Fig. 6b and the maxima values of $-\Delta S_M$ reach to 3.5 J/kg K and 6.9 J/kg K for the magnetic field changes from 0 to 2, and 5 T, respectively.

Another important parameter for magnetic refrigerant material is RC, which represents the amount of heat exchange between the cold and hot parts in a thermodynamic cycle. According to the calculation suggested by Gschneidner et al. [33], the values of RC are integrated by using the temperatures at the half-maximum of the peak as the integration limit [34–36]. The RC is defined as Eq. (3).

$$RC = \int_{T_{cold}}^{T_{hot}} |\Delta S_M| dT \quad (3)$$

T_{hot} and T_{cold} are the temperatures corresponding to the two sides of the half-maximum values of peak, respectively. The values of RC for Nd_3Pd_4 are calculated to be 25 J/kg and 74 J/kg for a field change of 0–2 and 0–5 T, respectively. Due to the incomplete $-\Delta S_M$-T curve, the values of RC for Pr_3Pd_4 are not given in the present work. For comparison, the MCE parameters of the R_3Pd_4 (R = Nd and Pr) compounds and some other refrigerant materials with a similar magnetic transition temperature are summarized in Table 1. It is evident that the values for the R_3Pd_4 (R = Nd and Pr) compounds are comparable to or larger than those magnetic refrigerant materials with a similar temperature region, indicating that the R_3Pd_4 (R = Nd and Pr) compounds could be a candidate for the magnetic refrigerator in low temperature range.

4 Conclusions

In summary, the magnetism and magnetocaloric effects of the R_3Pd_4 (R = Nd and Pr) compounds have been investigated experimentally. The Nd_3Pd_4 compound undergoes a magnetic transition from AFM to PM states at the Néel temperature $T_N = 9.4$ K. However, the AFM ground state shows a weak stability and can be easily induced to be FM state by an applied field. The Pr_3Pd_4 compound does not show any ordering under our experimental conditions. In the PM region, the reciprocal susceptibilities for both the compounds obey the Curie-Weiss law and the paramagnetic Curie temperatures (θp) for Nd_3Pd_4 and Pr_3Pd_4 were determined to be 6.5 K and − 17 K, with the corresponding effective magnetic moment (μ_{eff}) of 3.83 μ_B/Nd and 3.51 μ_B/Pr, respectively. For a field change of 5 T, the maximum values of $-\Delta S_M$ for Nd_3Pd_4 and Pr_3Pd_4 are determined to be 7.8 J/kg K and 6.9 J/kg K, respectively. The value of RC for Nd_3Pd_4 is evaluated to be 74 J/kg under the magnetic field change of 0–5 T.

Funding Information This work obtained financial support from the National Basic Research Program of China (Grant No. 2014CB643703), the National Natural Science Foundation of China (Grant No. 51801106), and Guangxi Natural Science Foundation, China (Grant No. 2018GXNSFAA294051, AD19110065). The authors also would like to thank K.C. Wong Magna Fund in Ningbo University.

References

1. Chen, J., Shen, B.G., Dong, Q.Y., Sun, J.R.: Solid State Commun. **150**, 1429–1431 (2010)
2. Pecharsky, V.K., Gschneidner Jr., K.A.: J. Magn. Magn. Mater. **200**, 44 (1999)
3. Tishin, A.M., Spichkin, Y.I.: In: Coey, J.M.D., Tilley, D.R., Vij, D.R. (eds.) The Magnetocaloric Effect and its Applications. Institute of Physics, London (2003)
4. Gschneidner Jr., K.A., Pecharsky, V.K., Tsokol, A.O.: Rep. Prog. Phys. **68**, 1479 (2005)
5. Niraj, K., Singh, P.K., Mao, Z., Paudyal, D., Neu, V., Suresh, K.G., Pecharsky, V.K., Gschneidner Jr., K.A.: J. Phys.: Condens. Matter. **21**, 456004 (2009)
6. Wang, X.J., Wang, L.J., Ma, Q.M., Sun, G., Zhang, Y.K., Cui, J.Z., Alloys, J.: Compd. **694**, 613–616 (2017)
7. Zhang, H., Shen, B.G., Xu, Z.Y., Shen, J., Hu, F.X., Sun, J.R., Long, Y.: Appl. Phys. Lett. **102**, 092401 (2013)
8. Chen, J., Shen, B.G., Dong, Q.Y., Hu, F.X., Sun, J.R.: Appl. Phys. Lett. **95**, 132504 (2009)
9. Chen, J., Shen, B.G., Dong, Q.Y., Sun, J.R.: Solid State Commun. **150**, 157–159 (2010)
10. de Campos, A., Rocco, D.L., Carvalho, A.M.G., Caron, L., Coelho, A.A., Gama, S., da Silva, L.M., Gandra, F.C.G., dos Santos, A.O., Cardoso, L.P., von Ranke, P.J., de Oliveira, N.A.: Nature Mater. **5**, 802 (2006)
11. Giguere, A., Foldeaki, M., Schnelle, W., Gmelin, E.: J. Phys. Condens. Matter. **11**, 6969 (1999)
12. Wada, H., Tomekawa, S., Shiga, M.: Cryogenics. **39**, 915 (1999)
13. Pecharsky, V.K., Gschneidner Jr., K.A.: Phys. Rev. Lett. **78**, 4494 (1997)

14. Pecharsky, V.K., Holm, A.P., Gschneidner Jr., K.A., Rink, R.: Phys. Rev. Lett. **91**, 197204 (2003)
15. Krenke, T., Duman, E., Acet, M., Wassermann, E.F., Moya, X., Manosa, L., Planes, A.: Nature Mater. **4**, 450 (2005)
16. Maji, B., Ray, M.K., Modak, M., Mondal, S., Suresh, K.G., Banerjee, S., Magn, J.: Mater. **456**, 236–240 (2018)
17. Zhang, H., Shen, B.G., Xu, Z.Y., Chen, J., Shen, J., Hu, F.X., Sun, J.R., Alloys, J.: Compd. **509**, 2602–2605 (2011)
18. Hu, W.J., Du, J., Li, B., Zhang, Q., Zhang, Z.D.: Appl. Phys. Lett. **92**, 192505 (2008)
19. Samanta, T., Das, I., Banerjee, S.: Appl. Phys. Lett. **91**, 152506 (2007)
20. Li, L.W., Nishimura, K., Yamane, H.: Appl. Phys. Lett. **94**, 102509 (2009)
21. Chen, J., Shen, B.G., Dong, Q.Y., Hu, F.X., Sun, J.R.: Appl. Phys. Lett. **96**, 152501 (2010)
22. Zhang, H., Wu, Y.Y., Long, Y., Wang, H.S., Zhong, K.X., Hu, F.X., Sun, J.R., Shen, B.G.: J. Appl. Phys. **116**, 213902 (2014)
23. Palenzona, A., Iandelli, A., Less-Common, J.: Met. **34**, 121–124 (1974)
24. Yakinthos, J.K., Gamari-Seale, H., Laforest, J.: Phys. Status Solidi. **40**, 105–108 (1977)
25. Singh, N.K., Suresh, K.G., Nirmala, R., Nigam, A.K., S. K., Malik, J.: Appl. Phys. **101**, 093904 (2007)
26. Niraj, K., Singh, K.G.S., Nirmala, R., Nigam, A.K., Malik, S.K.: J. Appl. Phys. **99**, 08K904 (2006)
27. Ehlers, G., Maletta, H.: Z. Phys. B. **99**, 145 (1996)
28. Mallik, R., Sampathkumaran, E.V., Paulose, P.L.: Solid State Commun. **106**, 169–172 (1998)
29. Wang, Y.X., Zhang, H., Wu, M.L., Tao, K., Li, Y.W., Yan, T., Long, K.W., Long, T., Pang, Z., Long, Y.: Chin. Phys. B. **25**, 127104 (2016)
30. Banerjee, B.K.: Phys. Lett. **12**, 16–17 (1964)
31. Tishin, A.M., Spichkin, Y.I.: The Magnetocaloric Effect and its Applications. IOP Publishing Ltd., Bristol (2003)
32. Mcmichael, R.D., Ritter, J.J., Shull, R.D.: J. Appl. Phys. **73**, 6946 (1993)
33. Gschneidner Jr., K.A., Pecharsky, V.K., Pecharsky, A.O., Zimm, C.B.: Mater. Sci. Forum. **69**, 315–317 (1999)
34. Franco, V., Borrego, J.M., Conde, A., Roth, S.: Appl. Phys. Lett. **88**, 132509 (2006)
35. Li, B., Hu, W.J., Liu, X.G., Yang, F., Ren, W.J., Zhao, X.G., Zhang, Z.D.: Appl. Phys. Lett. **92**, 242508 (2008)
36. Dong, Q.Y., Shen, B.G., Chen, J., Shen, J., Sun, J.R.: J. Appl. Phys. **105**, 113902 (2009)
37. Du, Y.S., Li, C.R., Cheng, G., Wu, X.F., Huo, J.J., Wei, J.Q., Wang, J., Supercond, J.: Novel Magn. **31**, 1–5 (2017)
38. Pecharsky, A.O., Mozharivskyj, Y., Dennis, K.W., Gschneidner Jr., K.A., McCallum, R.W., Miller, G.J., Pecharsk, V.K.: Phys. Rev. B. **68**, 134452 (2003)
39. Li, L.W., Nishimura, K.: J. Phys. D. Appl. Phys. **42**, 145003 (2009)
40. Ivtchenko, V.V., Pecharsky, V.K., Gschneidner Jr., K.A.: Adv. Cryog. Eng. **46**, 405 (2000)
41. Li, L.W., Nishimura, K., Usui, G., Huo, D.X., Qian, Z.H.: Intermetallics. **23**, 101–105 (2012)
42. Zhang, H., Xu, Z.Y., Zheng, X.Q., Shen, J., Hu, F.X., Sun, J.R., Shen, B.G.: J. Appl. Phys. **109**, 123926 (2011)
43. Li, L.W., Nishimura, K.: J. Appl. Phys. **106**, 023903 (2009)